

## Root pressure–volume curve traits capture rootstock drought tolerance

M. K. Bartlett<sup>1,\*</sup>, G. Sinclair<sup>1</sup>, G. Fontanesi<sup>1</sup>, T. Knipfer<sup>1,2</sup>, M. A. Walker<sup>1</sup> and A. J. McElrone<sup>1,3</sup>

<sup>1</sup>Department of Viticulture & Enology, University of California, Davis, CA 95616, USA, <sup>2</sup>Faculty of Land and Food Systems, The University of British Columbia, Vancouver, British Columbia V6T 1Z4, Canada and <sup>3</sup>USDA-ARS, Crops Pathology and Genetics Research Unit, Davis, CA 95616, USA

\*For correspondence. [mkbartlett@ucdavis.edu](mailto:mkbartlett@ucdavis.edu)

Received: 3 September 2021 Returned for revision: 12 October 2021 Editorial decision: 14 October 2021 Accepted: 18 October 2021

- **Background and Aims** Living root tissues significantly constrain plant water uptake under drought, but we lack functional traits to feasibly screen diverse plants for variation in the drought responses of these tissues. Water stress causes roots to lose volume and turgor, which are crucial to root structure, hydraulics and growth. Thus, we hypothesized that root pressure–volume (p–v) curve traits, which quantify the effects of water potential on bulk root turgor and volume, would capture differences in rootstock drought tolerance.
- **Methods** We used a greenhouse experiment to evaluate relationships between root p–v curve traits and gas exchange, whole-plant hydraulic conductance and biomass under drought for eight grapevine rootstocks that varied widely in drought performance in field trials (101-14, 110R, 420A, 5C, 140-Ru, 1103P, Ramsey and Riparia Gloire), grafted to the same scion variety (*Vitis vinifera* ‘Chardonnay’).
- **Key Results** The traits varied significantly across rootstocks, and droughted vines significantly reduced root turgor loss point ( $\pi_{\text{tlp}}$ ), osmotic potential at full hydration ( $\pi_o$ ) and capacitance ( $C$ ), indicating that roots became less susceptible to turgor loss and volumetric shrinkage. Rootstocks that retained a greater root volume (i.e. a lower  $C$ ) also maintained more gas exchange under drought. The rootstocks that previous field trials have classified as drought tolerant exhibited significantly lower  $\pi_{\text{tlp}}$ ,  $\pi_o$  and  $C$  values in well-watered conditions, but significantly higher  $\pi_o$  and  $\pi_{\text{tlp}}$  values under water stress, than the varieties classified as drought sensitive.
- **Conclusions** These findings suggest that acclimation in root p–v curve traits improves gas exchange in persistently dry conditions, potentially through impacts on root hydraulics or root to shoot chemical signalling. However, retaining turgor and volume in previously unstressed roots, as these roots deplete wet soil to moderately negative water potentials, could be more important to drought performance in the deep, highly heterogenous rooting zones which grapevines develop under field conditions.

**Key words:** Root hydraulics, pressure–volume, turgor loss point, capacitance, rootstock, grapevine, root drought tolerance, *Vitis*.

### INTRODUCTION

Roots are a significant bottleneck for water transport in droughted plants. The root system and soil–root interface account for 50–70 % of plant hydraulic resistance in wet conditions, and up to 90 % under water stress (Jensen *et al.*, 1989; North and Nobel, 1995; Tsuda and Tyree, 1997; Rodriguez-Dominguez and Brodrigg, 2020). Radial water transport across the root cylinder is a larger contributor to root hydraulic resistance than axial transport through the xylem (Stuedle and Peterson, 1998), especially for water-stressed roots (Cuneo *et al.*, 2016; Rodriguez-Dominguez *et al.*, 2018). However, we lack traits to characterize drought responses in the root cylinder tissues that are feasible to measure across diverse plants, despite the potential importance to whole-plant drought tolerance. Pressure–volume (p–v) curves define traits that characterize tissue drought responses from the impacts of water stress on bulk turgor and water volume (Cheung *et al.*, 1975). Tissues with stronger declines in turgor and volume are expected to undergo more structural damage and growth inhibition during drought (Hsiao *et al.*, 1976). Leaf p–v curve traits are strongly

correlated with hydraulic function under drought (Bartlett *et al.*, 2016), but these traits are rarely measured for roots, and the root traits have never been evaluated for impacts on plant drought performance. Thus, we used eight grape rootstocks that vary widely in drought tolerance in field conditions to conduct a novel test of the relationships between the root p–v curve traits and vine gas exchange, plant hydraulic conductance and growth under water stress.

Pressure–volume curves are constructed by repeatedly measuring the water potential and volume for a dehydrating organ (Turner *et al.*, 1987), and interpolated to define six traits: the turgor loss point ( $\pi_{\text{tlp}}$ ), osmotic potential at full hydration ( $\pi_o$ ), relative water content at the turgor loss point (RWC<sub>tlp</sub>), capacitance ( $C$ ), cell wall modulus of elasticity ( $\epsilon$ ) and apoplastic fraction ( $a_f$ ) (Cheung *et al.*, 1975). Turgor, the pressure generated by water pushing outwards against cell walls, supports cell structure and drives cell expansion during growth (Hsiao *et al.*, 1976).  $\pi_{\text{tlp}}$  measures the water potential ( $\Psi$ ) at which turgor declines to zero. Roots with a more negative  $\pi_{\text{tlp}}$  lose turgor at a more negative  $\Psi$ , and thus are expected to maintain structural integrity and growth under drier conditions.  $\pi_{\text{tlp}}$

is largely determined by  $\pi_o$ , and roots with a more negative  $\pi_o$  would exhibit a higher cell solute concentration and more negative  $\pi_{tp}$  (Bartlett et al., 2012b).  $RWC_{tp}$  and  $C$  measure the effects of water stress on tissue water volume.  $RWC_{tp}$  is the percentage of saturated volume remaining at  $\pi_{tp}$ , and  $C$  is the slope of the relationship between volume and  $\Psi$  (Cheung et al., 1975). Roots with a larger  $RWC_{tp}$  would retain more water at  $\pi_{tp}$ , while roots with a higher  $C$  would lose more water for a given decline in  $\Psi$ , with potentially detrimental effects on root structure (North and Nobel, 1997). We excluded  $\varepsilon$  and  $a_p$  since calculating these traits requires distinguishing water loss from the symplast and apoplast, and roots typically lose water from both sources simultaneously (Kandiko et al., 1980). Overall, we expect the rootstocks with a more negative  $\pi_{tp}$  and  $\pi_o$ , lower  $C$  and higher  $RWC_{tp}$  to better maintain root structure and function under water stress.

Several mechanisms could relate root turgor and volume, and, consequently, the p–v curve traits, to whole-plant drought performance. First, losing water from the cells causes dehydrating roots to shrink, physically decoupling the roots from the soil, and upregulates abscisic acid (ABA) production (Zhang and Tardieu, 1996; North and Nobel, 1997). Shrinkage in the root maturation zone, the band of root tissue chiefly responsible for water uptake, reduces hydraulic conductance at the soil–root interface (Carminati et al., 2009; Gambetta et al., 2013). Further, ABA export from the roots has been hypothesized to trigger stomatal closure (Speirs et al., 2013), though work in other species suggests that the stomata mainly respond to leaf ABA production (McAdam et al., 2016). Both mechanisms suggest that rootstocks that retain more root volume, with a higher  $RWC_{tp}$  and lower  $C$ , would maintain greater whole-plant hydraulic conductance and gas exchange under water stress. Second, water stress triggers the destruction of individual cells (cell implosion) in the maturation zone of grape roots. During implosion, the cell walls and membranes rupture, leaving air-filled lacunae in the root tissue that reduce conductivity by eliminating pathways for water movement (Cuneo et al., 2016, 2021). Cell implosion could release water from the root tissue, and thus a higher  $RWC_{tp}$  and lower  $C$  could indicate roots with less lacunae formation and smaller declines in conductivity. Further, the drivers of cell implosion are largely unknown, but turgor loss and wall collapse could be precipitating events, suggesting that a more negative  $\pi_{tp}$  and  $\pi_o$  could indicate that roots undergo lacunae formation at more negative water potentials. Finally, the rootstocks classified as drought tolerant by field trials exhibit more root growth than drought-sensitive varieties (Bauerle et al., 2008a), and a more negative root  $\pi_o$  has been shown to improve turgor and growth under water stress (Frensch and Hsiao 1994).

The widespread occurrence of osmotic adjustment suggests that plasticity in these traits is also important to drought tolerance. During drought, many grasses, herbs and woody plants, including grapevines, accumulate solutes (osmotically adjust) to make root  $\pi_o$ , and thus  $\pi_{tp}$ , more negative, allowing roots to maintain greater turgor and growth (Düring, 1984; Westgate and Boyer, 1985; Turner et al., 1987; Frensch and Hsiao, 1994; Knipfer et al., 2020). Two desert succulent species were also shown to decrease root  $C$  under water stress (Jordan and Nobel, 1984). Here we tested, for the first time, whether plasticity in these traits predicts rootstock differences in gas exchange and whole-plant hydraulic conductance during drought.

Finally, we tested whether these traits predict rootstock differences in field drought tolerance. We evaluated differences between drought-tolerant (110R, 1103P, Ramsey and 140-Ru) and drought-sensitive (101-14, 420A, 5C and Riparia Gloire) rootstocks, grafted onto the same scion variety (Chardonnay) to reduce variation in above-ground traits. The varieties classified as tolerant maintained greater canopy growth in low-irrigation field trials (Dodson Peterson et al., 2019). Grapevines are deeply rooted (approx. 2 m), and typically experience wet conditions in deeper soil and dry conditions at the surface at the same time, suggesting that trait values from wet and dry conditions are both potentially important to field drought performance (Smart et al., 2006; Bauerle et al., 2008a; Alsina et al., 2011). Overall, we expect this work to provide new insight into the impacts of drought responses in the living root tissues, captured by the root p–v curve traits, on whole-plant drought tolerance. These findings would also be the first to evaluate whether selecting for these traits is a promising strategy to improve rootstock drought tolerance.

## MATERIALS AND METHODS

### *Plant material and growth conditions*

Four drought-tolerant (110R, 1103P, 140-Ru and Ramsey) and four drought-sensitive grape rootstock varieties (5C, 420A, Riparia Gloire and 101-14) were grafted onto Chardonnay scions, using disease-free plant material supplied by the University of California, Davis Foundation Plant Services (Bettiga, 2003). Twenty plants per variety ( $n = 160$  total) were planted in 1.7 gallon pots on 18 June 2019, in a 3:1 coconut coir to perlite mix. Plants were grown in a greenhouse on the UC Davis campus over a 3 month establishment period (June to September) and a 3 month experimental period (September to December). During the establishment period, the vines were pruned to a single shoot, which was staked and tied after reaching 0.5 m in length. The new growth was tied monthly. Pots were watered with a nutrient infusion once every 2 weeks (see Knipfer et al., 2015 for nutrient composition), and otherwise with deionized water.

### *Watering treatments and whole-plant transpiration*

The pots were weighed and re-watered three times per week to a target weight (Supplementary data Fig. S1). During the establishment period, the target weight was equal to 95 % of the saturated pot weight plus half of pot evapotranspiration, to produce a mean pot water content between waterings that is approximately equal to 95 % of saturated pot weight (Pita and Pardos, 2001). Saturated weight was determined for each pot by adding water until drainage was visible and weighing the pot once water had been lost to the point that drainage had stopped. Plant evapotranspiration ( $E_{tot}$ ) was calculated as the change in pot weights (Supplementary data Fig. S2). Pot saturated weight and evapotranspiration were measured at the start of the establishment and experimental periods.

Half of the vines were randomly assigned to each of two watering treatments on 9 September. The well-watered vines continued to receive the same watering regime, while the

water-stressed vines were re-watered to 40 % of saturated pot mass, plus half of pot evapotranspiration under the new watering regime. Water was withheld from these vines until the pots reached 40 % of saturated mass, and the new evapotranspiration values were calculated from the difference in pot weights.

All plants were rehydrated overnight at the end of the experimental period (8 December). Most of the plants were then destructively harvested for biomass (see below), but three plants per rootstock  $\times$  treatment combination were weighed again to test the effects of the root p–v curve traits on the recovery in transpiration rates after drought.

### Root pressure–volume curves

Two to four vines per rootstock  $\times$  treatment combination were destructively harvested to construct p–v curves for two to three roots per vine ( $n = 108$  curves) (Fig. 1; Supplementary data Fig. S3). Water-stressed vines were measured after 20 September, when the pots reached the new target weights. Plants were rehydrated by watering until drainage was visible, then placing the vine and pot in a humidified bag overnight. The root systems were then rinsed. Individual roots were wiped dry and excised 15–20 cm above the root tip with a razor blade. Roots were stored in double bags, which were humidified by placing wet paper towel in the outer bag, in a refrigerator for up to 72 h. We confirmed that the roots did not dehydrate (i.e. initial water potentials remained above  $-0.1$  MPa) or discolour during storage. The outer bag was removed during measurements to prevent evaporation from the paper towel from affecting the mass values. To construct the curves, each root was removed from the bag to dehydrate between repeated measurements of root mass and water potential ( $\Psi$ ), following the methods in Sack and Pasquet-Kok (2011). After dehydrating, we closed the root in the bag for 10 min to allow  $\Psi$  to equilibrate, and weighed the bagged root. Root water potential was then measured with a pressure chamber (PMS model 1505D) by monitoring the cut root surface through a dissecting scope, as the chamber was

slowly pressurized (approx.  $0.05$  MPa  $s^{-1}$ ) until water emerged. The cut end was threaded through a rubber stopper with a narrow opening (3 mm in diameter) to create a tight seal, using a cork borer when needed to avoid damaging the root. The rest of the root was placed in the bag to prevent drying during the pressure chamber measurements. These measurements were repeated 6–10 times per root at approx. 0.1–0.3 MPa intervals. The roots were then oven-dried at  $70$  °C for 72 h, and the dry weights were used to calculate relative water content (RWC), the ratio of fresh to saturated water mass.

The p–v curve traits were interpolated from these relationships following standard methods (Sack and Pasquet-Kok, 2011). The turgor loss point ( $\pi_{\text{tlp}}$ ) and relative water content at turgor loss point ( $\text{RWC}_{\text{tlp}}$ ) were defined graphically, as the water potential and relative water content at which the relationship between RWC and  $-1/\Psi$  transitioned from curvilinear to linear. The linear relationship between RWC and  $-1/\Psi$  was extrapolated to  $\text{RWC} = 1$  to calculate the osmotic potential at full hydration ( $\pi_o$ ). Capacitance was defined as the slope of the relationship between RWC and  $\Psi$ . We calculated capacitance separately for water potentials above and below  $\pi_{\text{tlp}}$  (i.e.  $C_{\text{ft}}$  and  $C_{\text{tp}}$ ), since turgor pressure generally decreases capacitance by supporting the cell walls and providing resistance against changes in cell volume.

### Gas exchange, water status and whole-plant hydraulic conductance

Three vines per rootstock  $\times$  treatment combination ( $n = 48$ ) were assessed for gas exchange and water stress, measured as midday leaf water potentials ( $\Psi_{\text{md}}$ ), every 2–3 weeks (see Supplementary data Figs S4–S6 for a timeline of these measurements). The gas exchange measurements were taken on two consecutive days to capture variation in the period between waterings. These variables were measured at the hottest and thus most water-stressed time of the day in the greenhouse, between 13.00 and 15.00 h. One sunlit, fully expanded leaf per vine was marked and repeatedly measured for stomatal conductance ( $g_s$ )

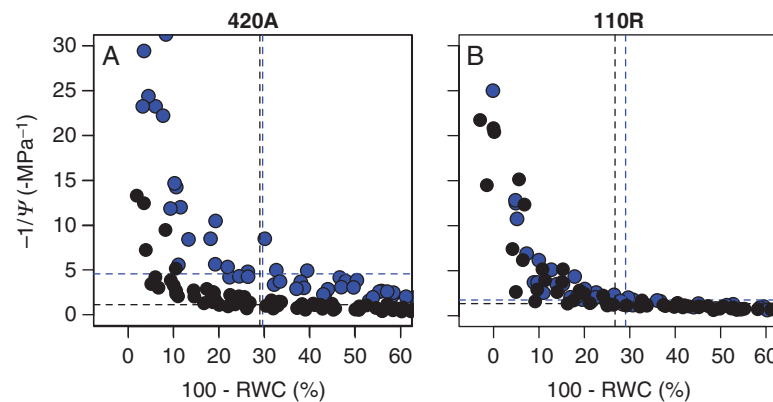


FIG. 1. Root pressure–volume curve examples from two of the most distinct rootstock varieties, 420A (A) and 110R (B). RWC is root relative water content and  $\Psi$  is root water potential. Blue points and lines show well-watered plants, and black points and lines show water-stressed plants. Horizontal lines indicate the mean turgor loss point ( $\pi_{\text{tlp}}$ ,  $y = -1/\pi_{\text{tlp}}$ ) and vertical lines indicate the mean relative water content at  $\pi_{\text{tlp}}$  ( $\text{RWC}_{\text{tlp}}$ ,  $x = 100 - \text{RWC}_{\text{tlp}}$ ).  $n = 6$ –7 roots per rootstock/treatment combination. 420A exhibited a less negative  $\pi_{\text{tlp}}$  than 110R under well-watered conditions but adjusted to a more negative  $\pi_{\text{tlp}}$  under water stress, while  $\text{RWC}_{\text{tlp}}$  was similar between treatments and rootstocks. Field trials have classified 420A as drought sensitive and 110R as tolerant (Dodson Peterson *et al.*, 2019). See Supplementary data Fig. S3 for curves from all eight rootstocks.

and photosynthesis ( $A_{\text{net}}$ ) with a LI-COR 6800 photosynthesis system (Supplementary data Figs S4 and S5). The LI-COR was set at a constant fan speed (10 000 rpm), chamber vapour pressure deficit (1.5 kPa),  $\text{CO}_2$  concentration (400 ppm) and light intensity ( $1000 \mu\text{mol m}^{-2} \text{s}^{-1}$ ). The leaf temperature ranged from 26.5 to 27.5 °C.

To measure  $\Psi_{\text{md}}$ , one leaf per vine was excised with a razor blade from a similar canopy position to the gas exchange leaves (Supplementary data Fig. S6). The leaves were stored in humidified double bags in a refrigerator for up to 24 h, then measured for water potential with the pressure chamber. On two of the sampling dates, 4 and 12 November, leaves were collected from the same vines between 04.00 and 06.00 h to measure pre-dawn water potential ( $\Psi_{\text{pd}}$ ), which we assumed to represent the water potential of the rooting zone.

To test the effects of the root p–v curve traits on plant hydraulics, we used the water potential gradient and evapotranspiration to calculate the whole-plant hydraulic conductance as  $K_{\text{plant}} = \frac{E_{\text{tot}}}{\Psi_{\text{pd}} - \Psi_{\text{md}}}$ . To distinguish the effects of root hydraulic resistance and root system size, we also calculated  $K_{\text{RA}}$ , or  $K_{\text{plant}}$  normalized by root system area. We measured these variables close to the date of the biomass harvest (9 December, see below) to accurately capture root area.

We also used  $\Psi_{\text{pd}}$  to calculate two drought response variables incorporating differences in below-ground water stress across the individual plants. We calculated a root hydraulic safety margin ( $\text{HSM} = \Psi_{\text{pd}} - \pi_{\text{tup}}$ ) from the  $\Psi_{\text{pd}}$  measured for each plant and the mean  $\pi_{\text{tup}}$  for each rootstock × treatment combination ( $n = 48$ ). A larger positive HSM indicates the plants maintain greater turgor, with a larger safety margin between the below-ground water potential and the threshold for turgor loss. We calculated a percentage volumetric water loss (WL) from the  $\Psi_{\text{pd}}$  measured for each plant and the mean root capacitance values

$$\text{WL} = \begin{cases} C_{\text{fit}} \Psi_{\text{PD}} & \Psi_{\text{PD}} > \pi_{\text{tup}} \\ C_{\text{fit}} \pi_{\text{tup}} + C_{\text{tup}} (\pi_{\text{tup}} - \Psi_{\text{PD}}) & \Psi_{\text{PD}} \leq \pi_{\text{tup}} \end{cases} \quad (1)$$

where a larger WL indicates greater root water loss. We compared relationships with gas exchange for these variables and the p–v traits, to evaluate whether differences in plant water stress within the experiment were important to whole-plant drought responses.

#### Canopy and root system size

We measured the canopy surface area for all plants at the end of the experimental period (9 December). The plants were photographed with an imaging platform designed by T. Knipfer, consisting of a PVC frame that holds a camera at a standard distance and angle from each pot. The plants were photographed from the front and side, then we used the thresholding function in the ImageJ software to isolate and quantify the canopy area for each photograph (Schneider *et al.*, 2012). We calculated the mean canopy area for each plant from the front and side photographs. Notably, this method does not distinguish between overlapping leaves, and thus measures surface and not total leaf area.

We also destructively harvested the plants that were not monitored for gas exchange to measure above- and below-ground biomass on the same day ( $n = 76$ ). The plants were cut at the soil surface and the root systems were rinsed. Three roots per rootstock × treatment combination were excised at the stem, photographed, and measured for area with ImageJ. These roots were then oven-dried at 70 °C for 3 d and weighed to calculate root mass per unit area. The scions and rest of the root systems were also oven-dried at 70 °C for 4 weeks and weighed. The individual root masses were added to the rest of the root system biomass for each plant. The root biomasses and mass per area values were used to estimate the total root area for each plant.

The plants measured for gas exchange were rewatered to 100 % of saturated pot weight on 9 December to monitor recovery in transpiration, then destructively harvested following the same methods on 16 December ( $n = 48$ ). The biomass data from the two sampling dates were statistically indistinguishable, and so were pooled for the following analyses ( $n = 124$ ).

#### Analyses

We first tested whether the root p–v curve traits and their responses to water stress were significantly different among the rootstock varieties. We fit each trait with the linear mixed-effects model  $y \sim \text{Treatment} \times \text{Variety}$  using the nlme package in R (v. 3.6.2). We modelled the watering treatment and rootstock variety as fixed effects and the individual plant as a random effect. We evaluated the support for each fixed effect as a predictor by conducting an AICc comparison among models with all possible combinations of the fixed-effect variables, using the ‘dredge’ function in the package MuMIN (Barton, 2009). AICc values are Aikake information criterion corrected for small sample sizes (Burnham and Anderson, 2010). We defined the best-fit model as the model with the minimum AICc value or, where applicable, the most parsimonious sub-set of this model with an AICc value within 2 units of the minimum (Burnham and Anderson, 2010). We determined goodness-of-fit for the best-fit model by calculating the proportion of variation explained by the entire model (conditional  $r^2$ ) and the fixed effects alone (marginal  $r^2$ ) (Nakagawa and Schielzeth, 2013).

We then tested the impact of the root p–v curve traits on gas exchange ( $g_s$ ,  $A_{\text{net}}$  and  $E_{\text{tot}}$ ), water status ( $\Psi_{\text{md}}$ ) and whole-plant hydraulic conductance ( $K_{\text{plant}}$  and  $K_{\text{RA}}$ ) by fitting these variables with the linear mixed-effects model  $y \sim \text{Treatment} \times \text{Time} \times \text{Trait}$ . We only included the gas exchange and  $\Psi_{\text{md}}$  data from 20 September to 8 December to allow the water-stressed plants time to adjust trait values to the new conditions (Düring, 1984). We modelled the watering treatment, number of days after the start of the experimental period (Time), either a trait variable or the rootstock variety (Trait), and their interaction terms as fixed effects. We included the individual plant as a random effect. We first used AICc comparisons to identify the best-fit model for each trait variable, then ranked these models to compare predictive ability across traits.

Since the gas exchange and  $\Psi_{\text{md}}$  measurements were repeated over time, we also tested for temporal autocorrelation in these data. We repeated the AICc comparisons for the same models while also including a first-order autoregressive correlation structure, using the ‘corCAR0031’ function in nlme. AICc

comparisons between the models with and without this correlation structure only supported including autocorrelation in the best-fit model for  $E_{\text{tot}}$ . We also used this model to test whether rootstock differences in gas exchange reflect differences in both traits and the degree of water stress, by including the percentage root water loss (WL) and hydraulic safety margin (HSM) as Trait predictors.

We used the same methods to test for an effect of the root traits on hydraulic recovery from drought by fitting the model  $E_{\text{tot, recovery}} \sim E_{\text{tot, pre-recovery}} \times \text{Treatment} \times \text{Trait}$ , where  $E_{\text{tot, pre-recovery}}$  and  $E_{\text{tot, recovery}}$  are the evapotranspiration rates measured immediately before and after rehydration (i.e. on 7 and 9 December). We also tested for an effect of the root traits on plant size by fitting the model  $y \sim \text{Treatment} \times \text{Trait}$  to the above- and below-ground biomass and area.

Finally, we evaluated trait variation between drought-tolerant and -sensitive rootstocks varieties by testing the two-way analysis of variance (ANOVA)  $y \sim \text{Treatment} \times \text{Drought Tolerance Category}$  for each trait variable. We defined the varieties with low to medium tolerance in field trials as drought sensitive (i.e. 420A, 5C, Riparia Gloire and 101-14) and the varieties with medium/high to high tolerance as drought tolerant (i.e. 110R, 1103P, 140Ru and Ramsey) (Bettiga, 2003).

## RESULTS

### *Root p–v curve traits varied across rootstocks and adjusted in response to water stress*

All of the root p–v curve traits except  $\text{RWC}_{\text{tip}}$  varied across the eight rootstocks (Table 1; Figs 1 and 2; Supplementary data Fig. S3). Three traits,  $\pi_{\text{tip}}$ ,  $\pi_{\text{o}}$  and  $C_{\text{ft}}$ , also adjusted to lower values under water stress, and the magnitude of this adjustment varied across the rootstocks (Table 1; Figs 1 and 2; Supplementary data Fig. S3). These trends were inferred from AICc comparisons, which identified rootstock variety, watering treatment and the interaction of rootstock  $\times$  treatment as best-fit predictors for  $\pi_{\text{tip}}$ ,  $\pi_{\text{o}}$  and  $C_{\text{ft}}$ , but only rootstock variety as a best-fit predictor for  $C_{\text{tip}}$ , and neither variable as a best-fit predictor for  $\text{RWC}_{\text{tip}}$  (Table 1). These findings suggest that grape rootstocks vary strongly in the ability to retain bulk tissue turgor and volume in water-stressed

roots, and that both constitutive trait variation and plasticity are important to rootstock differences in drought tolerance.

### *Root p–v curve traits were related to gas exchange under water stress*

Root p–v curve traits were correlated with midday stomatal conductance ( $g_s$ ), photosynthesis ( $A_{\text{net}}$ ) and daily whole-plant transpiration ( $E_{\text{tot}}$ ) under water stress (Table 2; Figs 3–5). The AICc comparisons identified the watering treatment, time during the experimental period and root capacitance traits as best-fit predictors for  $g_s$  and  $A_{\text{net}}$  (Table 2). Water stress reduced  $g_s$  and  $A_{\text{net}}$ , and both variables declined over the course of the experiment as the leaves aged (Figs 3 and 4; Supplementary data Figs S4 and S5). The rootstocks with a lower capacitance, measured at water potentials above and below the turgor loss point ( $C_{\text{ft}}$  and  $C_{\text{tip}}$ ), maintained a higher  $g_s$  under water stress (Fig. 3D, E). These relationships were strongest in the water-stressed treatment, while  $C_{\text{tip}}$  had no impact, and  $C_{\text{ft}}$  had the opposite effect, on  $g_s$  in well-watered conditions. A lower  $C_{\text{ft}}$  was also associated with a higher  $A_{\text{net}}$ , as for  $g_s$ , and this relationship was also stronger under water-stressed conditions (Fig. 4D). These findings suggest that maintaining root volume benefits gas exchange and water uptake from the soil under water stress.

Whole-plant transpiration ( $E_{\text{tot}}$ ) also declined under water stress and over the course of the experiment (Fig. 5; Supplementary data Fig. S2) but showed different relationships with the root p–v curve traits (Fig. 5).  $E_{\text{tot}}$  was higher for the rootstocks with a lower  $C_{\text{tip}}$  and more negative  $\pi_{\text{tip}}$ , but these traits had greater impacts on transpiration under well-watered conditions, while rootstocks converged on similar transpiration rates under water stress (Table 2; Fig. 5A, E). These findings appear to reflect trends in canopy size.  $E_{\text{tot}}$  was significantly correlated with both  $g_s$  and canopy surface area ( $r^2 = 0.80$ ,  $P < 0.001$ ), but more strongly with canopy area (partial  $r^2 = 0.26$  and  $0.81$ , respectively). The rootstocks produced similar canopy areas within each watering treatment, with especially little variation under water stress (Fig. 6B). Thus, despite differences in  $g_s$ , the water-stressed rootstocks converged on a similar mean  $E_{\text{tot}}$ , ranging from  $0.09$  to  $0.10 \text{ kg d}^{-1}$ , compared with  $0.16$  to  $0.27 \text{ kg d}^{-1}$  for the well-watered plants (Fig. 5).

TABLE 1. Best-fit models predicting the root pressure–volume curve traits turgor loss point ( $\pi_{\text{tip}}$ ), osmotic potential at full hydration ( $\pi_{\text{o}}$ ), relative water content at turgor loss point ( $\text{RWC}_{\text{tip}}$ ), capacitance from full hydration to turgor loss point ( $C_{\text{ft}}$ ) and capacitance at water potentials below turgor loss point ( $C_{\text{tip}}$ )

	$\pi_{\text{tip}}$ (MPa)	$\pi_{\text{o}}$ (MPa)	$\text{RWC}_{\text{tip}}$ (%)	$C_{\text{ft}}$ (% $\text{MPa}^{-1}$ )	$C_{\text{tip}}$ (% $\text{MPa}^{-1}$ )
Intercept	−0.42	−1.01	74.6	0.52	0.66
Rootstock	*	*	*	*	*
Treatment	−0.56	−0.14		−0.15	
Treatment $\times$ Rootstock	*	*		*	
Marginal $r^2$	0.68	0.64	0	0.56	0.23
Conditional $r^2$	0.70	0.65	0.15	0.59	0.24

We used AICc comparisons to identify the best-fit model for each trait from all possible sub-sets of the full model including watering treatment, rootstock variety and the interaction between treatment and variety as fixed effect predictors ( $n = 6$ – $10$  roots per rootstock  $\times$  treatment combination). The individual plant was included as a random effect. The fitted parameter values are shown for the predictors included in the best-fit model. For brevity, best-fit predictors with multiple categories (i.e. rootstock variety) are indicated with an asterisk. Marginal  $r^2$  indicates the proportion of variance explained by the fixed effects, and conditional  $r^2$  indicates the variance explained by both fixed and random effects.

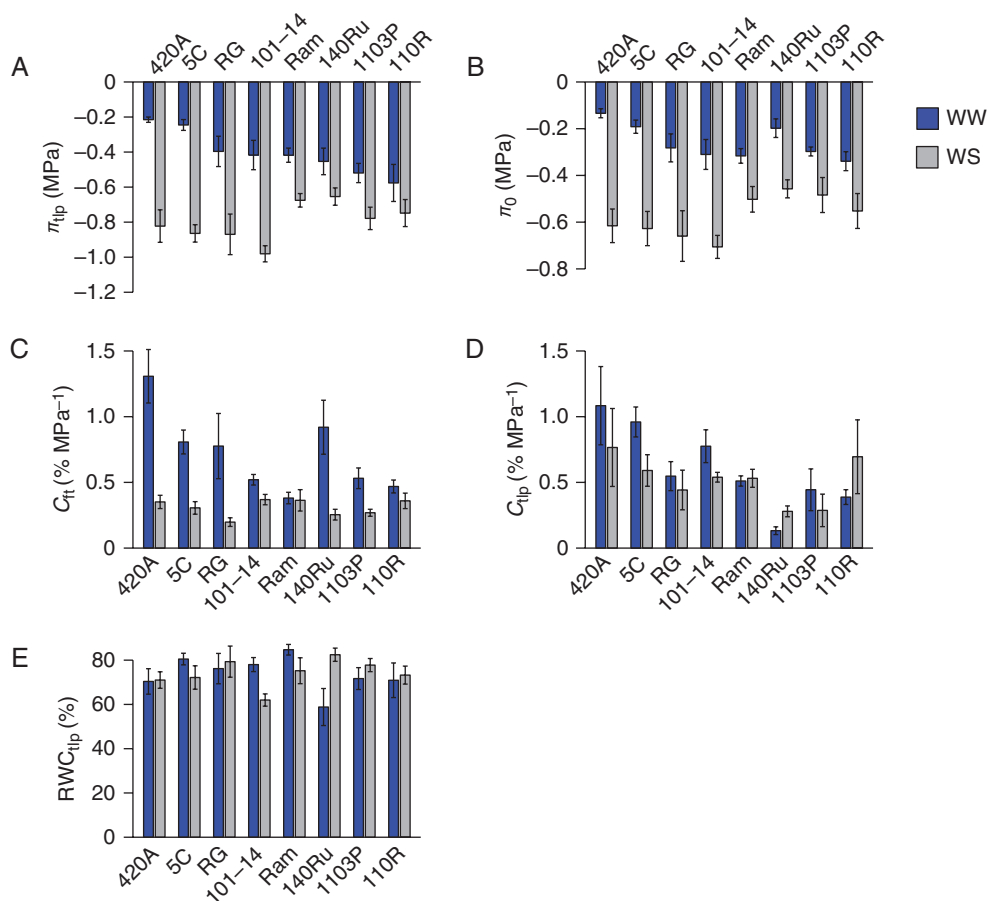


FIG. 2. Mean root turgor loss point ( $\pi_{tip}$ ) (A), osmotic potential at full hydration ( $\pi_0$ ) (B), capacitance between full hydration and turgor loss point ( $C_{fit}$ ) (C), capacitance for water potentials below turgor loss point ( $C_{tip}$ ) (D) and relative water content at turgor loss point ( $RWC_{tip}$ ) (E) for each of the 16 rootstock variety  $\times$  watering treatment combinations. Blue bars indicate well-watered and grey bars indicate water-stressed conditions. Error bars are standard errors ( $n = 5-11$ ). All of the root pressure–volume curve traits except  $RWC_{tip}$  varied across the rootstocks, and all traits except  $RWC_{tip}$  and  $C_{tip}$  were significantly reduced in the water-stressed plants (Table 1).

TABLE 2. The best-fit models predicting gas exchange, including midday stomatal conductance ( $g_s$ ) and photosynthesis ( $A_{net}$ ) and daily whole-plant transpiration ( $E_{tot}$ ), from the root pressure–volume curve traits

	Trait	$a$	$b$	$c$	$d$	$e$	$f$	Mar. $r^2$	Cond. $r^2$	$\Delta AICc$
$g_s$	$C_{fit}$	146	115	85	*	*	-540	0.45	0.73	-6.3
	WL	176	102	57	*	*	-642	0.41	0.73	-3.9
	$C_{tip}$	228	2.9	-53	*	*	-146	0.41	0.73	-2.4
$A_{net}$	$C_{fit}$	6.5	0.6	7.2	*	*	-27	0.31	0.73	-3.9
	WL	6.5	1.8	3.0	*	*	-32	0.30	0.73	-3.4
$E_{tot}$	Variety	0.43	*	-0.28	-0.003	0.002	*	0.63	0.85	-7.4
	$C_{tip}$	0.44	-0.03	-0.29	-0.003	0.002		0.61	0.85	-4.8
	$\pi_{tip}$	0.39	-0.09	-0.36	-0.003	0.002	0.08	0.61	0.85	-3.4
	HSM	0.41	0.13	-0.29	-0.003	0.002	-0.08	0.61	0.85	-3.1

We used AICc comparisons to identify the best-fit model for each trait from all possible sub-sets of the model  $a + b \times \text{Trait} + c \times \text{Treatment} + d \times \text{Time} + e \times \text{Treatment} \times \text{Time} + f \times \text{Treatment} \times \text{Treatment} \times \text{Treatment}$ . Here, we show the fitted parameters from the best-fit model for every trait that improved predictions for gas exchange, as defined by  $\Delta AICc$ .  $\Delta AICc$  is the difference in AICc values between the best-fit model for each trait and the best-fit model without trait predictors. The traits with a  $\Delta AICc < -2$  were considered to substantively improve predictions for gas exchange. For brevity, the best-fit predictors with multiple categories (e.g. rootstock variety) are indicated with asterisks. Time was represented as a continuous variable for  $E_{tot}$  and a categorical variable for  $g_s$  and  $A_{net}$ , since these variables were sampled less frequently.

The root p–v curve traits were also related to the increase in canopy transpiration after rehydrating pots to 100 % of saturated weight, compared with 40 and 95 % in the experimental

treatments (Supplementary data Table S1, Fig. S7). Plants with a higher transpiration rate in the 2 d before re-watering ( $E_{pre-recovery}$ ) also exhibited greater transpiration after re-watering

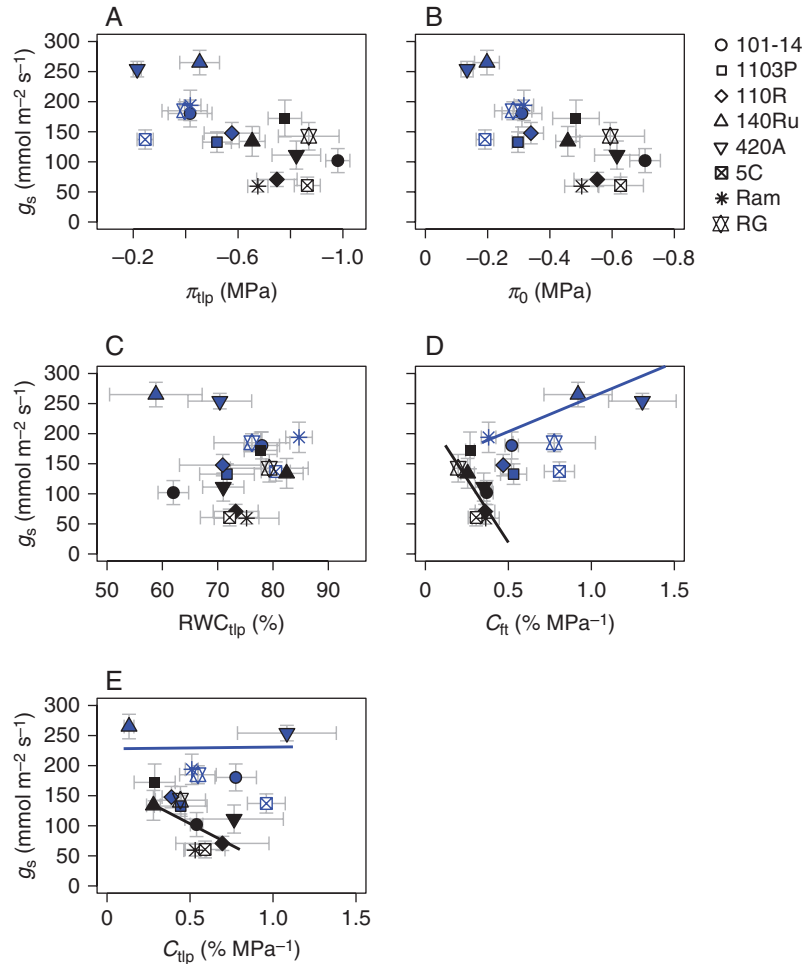


FIG. 3. Relationships between the root pressure–volume curve traits and mean midday stomatal conductance ( $g_s$ ) over the experimental period. Blue points indicate well-watered trait values and black points are water-stressed values. Field trials classified the rootstocks as drought tolerant and drought sensitive (Dodson Peterson *et al.*, 2019). Error bars are standard errors.  $n = 5–11$  roots for the p–v curve traits;  $n = 3$  plants for  $g_s$ .  $g_s$  was reduced by water stress and varied over time during the experiment (Supplementary data Fig. S3). AICc comparisons identified root capacitance, both above and below the turgor loss point ( $C_{fit}$  and  $C_{tip}$ ), as well-supported predictors for  $g_s$  (shown as solid lines) (Table 2). A lower  $C_{fit}$  and  $C_{tip}$ , which indicate that the roots retain a greater water volume for a given decline in water potential, were associated with a higher  $g_s$  under water stress, but had little or the opposite impact on  $g_s$  under well-watered conditions (D and E) (Table 2).

( $E_{recovery}$ ). However,  $E_{recovery}$  was still lower for water-stressed plants, even when controlling for  $E_{pre-recovery}$ . A higher  $C_{tip}$  and  $RWC_{tip}$  were associated with a higher transpiration rate when controlling for  $E_{pre-recovery}$ . However, these relationships appear to be driven by a high capacity for the unstressed plants from one variety (Riparia) to upregulate transpiration after watering, rather than a general trend for rootstocks with higher  $C_{tip}$  and  $RWC_{tip}$  to exhibit greater recovery from water stress (Supplementary data Fig. S7).

#### Root p–v curve traits were not related to plant water stress or hydraulic conductance

Contrary to expectation, the root p–v curve traits were not correlated with water stress or hydraulic conductance. The drought treatment reduced pre-dawn and midday leaf water potentials ( $\Psi_{pd}$  and  $\Psi_{md}$ ), whole-plant hydraulic conductance ( $K_{plant}$ ) and  $K_{plant}$  normalized by root area ( $K_{RA}$ ) (Supplementary

data Table S2; Fig. 7). Mean rootstock values for  $\Psi_{pd}$  and  $\Psi_{md}$  ranged from  $-0.22$  to  $-0.37$  MPa and  $-0.61$  to  $-0.77$  MPa in the well-watered treatment, and from  $-0.34$  to  $-0.45$  MPa and  $-0.74$  to  $-0.95$  MPa in the water-stressed treatment, respectively. The watering treatments were intended to impose the same level of stress on each variety and, consistent with this expectation,  $\Psi_{pd}$  and  $\Psi_{md}$  were not correlated with the root traits or different across rootstock varieties. Although not expected,  $K_{plant}$  was also not related to the root traits or different across varieties.  $K_{RA}$  varied significantly across rootstocks, but this trend appears to be driven by rootstock differences in root area, rather than hydraulic conductance (Supplementary data Table S2).

Both the p–v curve traits and the level of water stress in the rooting zone would impact root turgor and volume. Thus, we tested whether variables accounting for both traits and water stress, the hydraulic safety margin between  $\Psi_{pd}$  and  $\pi_{tip}$  (HSM) and the percentage water loss at  $\Psi_{pd}$  (WL), were more strongly related to gas exchange than to the traits alone. These variables

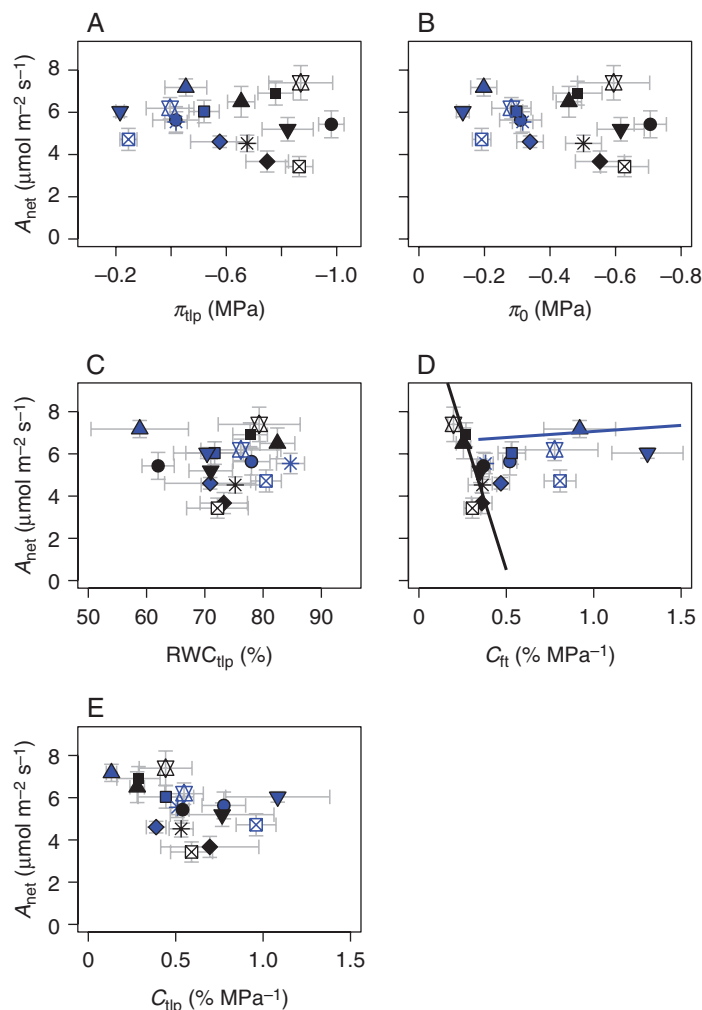


FIG. 4. Relationships between the root p–v curve traits and mean midday photosynthetic rates over the experiment ( $A_{\text{net}}$ ). Symbols follow Fig. 3.  $n = 5\text{--}11$  roots for the p–v traits;  $n = 3$  plants for  $A_{\text{net}}$ . As for  $g_s$ , a lower root capacitance at water potentials between full hydration and the turgor loss point ( $C_{\text{fit}}$ ) was associated with a higher  $A_{\text{net}}$  under water stress but had little impact on  $A_{\text{net}}$  under well-watered conditions (D) (Table 2). AICc comparisons did not support the other traits as predictors for  $A_{\text{net}}$ .

showed the same relationships as the traits, with minimal differences in the marginal  $r^2$  between best-fit models (i.e.  $<0.04$ ), consistent with the lack of strong differences in  $\Psi_{\text{pd}}$  (Table 2).

*Root p–v curve traits were related to the size of the root system, but not the canopy*

Water stress reduced both below- and above-ground growth, but the root p–v curve traits were only related to root system size (Table 3; Fig. 6). A larger root system biomass was associated with a lower  $\text{RWC}_{\text{tlp}}$ , while all of the root p–v curve traits were identified as predictors for root system area. A larger area was associated with a lower  $\text{RWC}_{\text{tlp}}$  and, as hypothesized, a more negative  $\pi_{\text{tlp}}$  and  $\pi_0$  and a lower  $C_{\text{fit}}$  and  $C_{\text{tlp}}$  (Table 3; Fig. 6A). However, root biomass and area were more strongly related to rootstock variety than to the individual traits (Table 3), suggesting that below-ground growth was determined by other rootstock factors. Water stress also reduced the canopy surface area and biomass, but the canopy size was not related to the root traits or rootstock variety (Table 3, Fig. 6B).

*Root p–v curve traits measured for well-watered plants captured differences in rootstock drought tolerance under field conditions*

Most of the root p–v curve traits were significantly different between the rootstocks classified as drought tolerant (140-Ru, 1103P, 110R and Ramsey) and drought sensitive (101-14, 420A, 5C and Riparia Gloire) by previous field trials. The drought-tolerant varieties exhibited significantly lower values for  $\pi_{\text{tlp}}$ ,  $\pi_0$ ,  $C_{\text{fit}}$  and  $C_{\text{tlp}}$ , but only for trait values measured under well-watered conditions, contrary to our expectations (ANOVA,  $P < 0.001$ ) (Fig. 8). The  $C_{\text{fit}}$  and  $C_{\text{tlp}}$  values measured under water stress were not significantly different between drought-tolerant and drought-sensitive varieties ( $P > 0.3$ ), while the  $\pi_{\text{tlp}}$  and  $\pi_0$  values were significantly less negative in the drought-tolerant varieties ( $P < 0.01$ ) (Fig. 8).

## DISCUSSION

This study is novel in showing that root p–v curve traits are important to whole-plant drought responses. These traits were significantly different across grape rootstocks, and adjusted

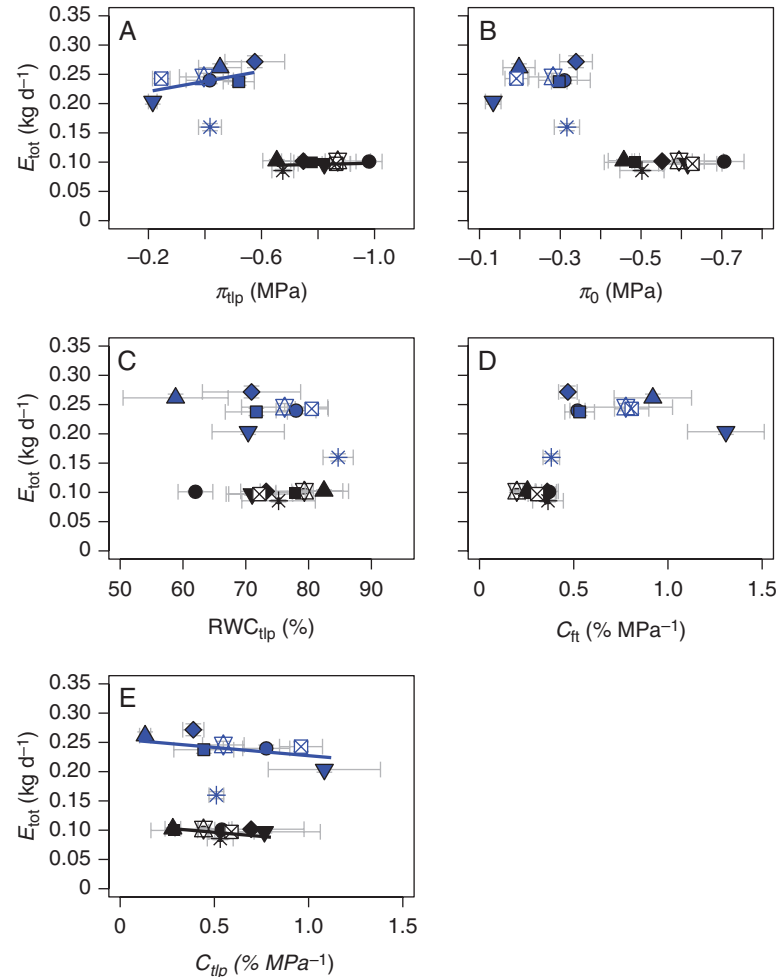


FIG. 5. Relationships between the root pressure–volume curve traits and mean daily whole-plant transpiration ( $E_{tot}$ ) over the experimental period. Symbols follow Fig. 3.  $n = 5$ –11 roots for the p–v traits;  $n = 8$ –10 plants for  $E_{tot}$ . As for  $g_s$  and  $A_{net}$ ,  $E_{tot}$  was reduced by water stress and varied over time (Supplementary data Fig. S2). Further, a lower root capacitance at water potentials below turgor loss point ( $C_{tip}$ ), and a more negative root turgor loss point ( $\pi_{tip}$ ), were associated with a higher  $E_{tot}$  (A, E) (Table 2). However, this relationship was stronger under well-watered conditions than under water stress, while the rootstocks converged on a similar  $E_{tot}$  under water stress (A, E).

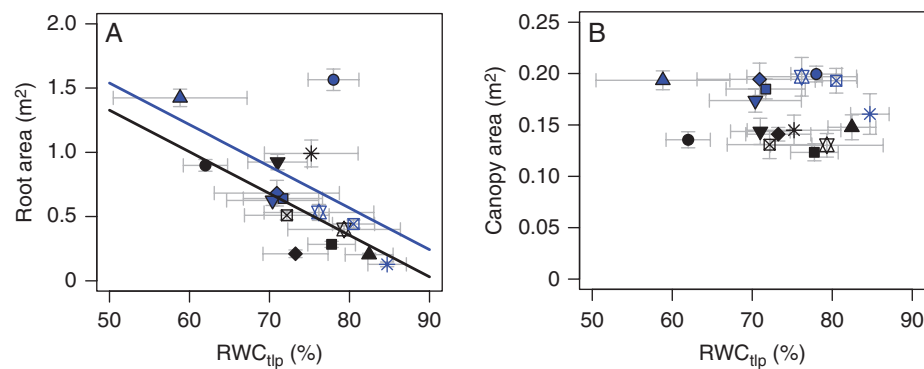


FIG. 6. Examples of the relationships between root p–v curve traits (here, relative water content at turgor loss point;  $RWC_{tip}$ ) and plant size, measured as canopy surface area (A) and root system area (B) at the end of the experimental period. Symbols follow Fig. 3.  $n = 5$ –11 roots for the p–v traits, 7–8 plants for canopy area and 4–5 plants for root system area. Water stress significantly reduced both canopy and root area, while only root area was related to the root p–v traits. All of the root traits significantly improved prediction for root area, but rootstock variety was a stronger predictor than any individual trait, suggesting that rootstock differences in root system size are mainly driven by other factors (Table 3).

to significantly lower values, which are expected to maintain greater root turgor and volume, under water stress (Figs 1 and 2; Supplementary data Fig. S3). Lower root capacitance, which

indicates that roots retain greater volume as water potentials decline, was significantly associated with greater gas exchange in the water-stressed plants (Figs 3 and 4). However, the rootstocks

TABLE 3. The best-fit models predicting plant size, measured as root system and canopy biomass and area at the end of the experimental period

	Trait	<i>a</i>	<i>b</i>	<i>c</i>	<i>d</i>	Mar. $r^2$	Cond. $r^2$	$\Delta\text{AICc}$
Root biomass	Variety	0.09	*	-0.03		0.49	0.94	-19.4
	RWC <sub>tip</sub>	0.16	-0.001	-0.1	0.001	0.36	0.92	-4.4
Root area	Variety	1.6	*	-0.67	*	0.89	0.98	-296.8
	RWC <sub>tip</sub>	3.2	-0.03	-0.21		0.33	0.92	-114.8
	$C_{tip}$	1.0	-0.38	-0.95	1.3	0.32	0.92	-88.9
	$C_{ft}$	0.79	0.003	-1.2	3.1	0.18	0.90	-88.3
	$\pi_{tip}$	0.42	-0.92	-0.62		0.14	0.89	-87.3
	$\pi_o$	0.54	-0.99	-0.56		0.12	0.89	-81.9
	—	—	—	—	—	—	—	—
Canopy biomass	—	0.05	—	-0.01	—	0.16	0.90	0
Canopy area	—	0.19	—	-0.05	—	0.38	0.92	0

The best-fit model for each trait was identified from all possible sub-sets of the model  $a + b \times \text{Trait} + c \times \text{Treatment} + d \times \text{Treatment} \times \text{Trait}$ . Fitted parameters are shown for the best-fit model for each trait that improved predictions for plant size, defined as an  $\Delta\text{AICc} < -2$ , compared with the best-fit model without trait predictors. None of the trait variables substantively improved predictions for canopy size (indicated with ‘—’ in the Trait variable column). Other symbols follow Table 2.

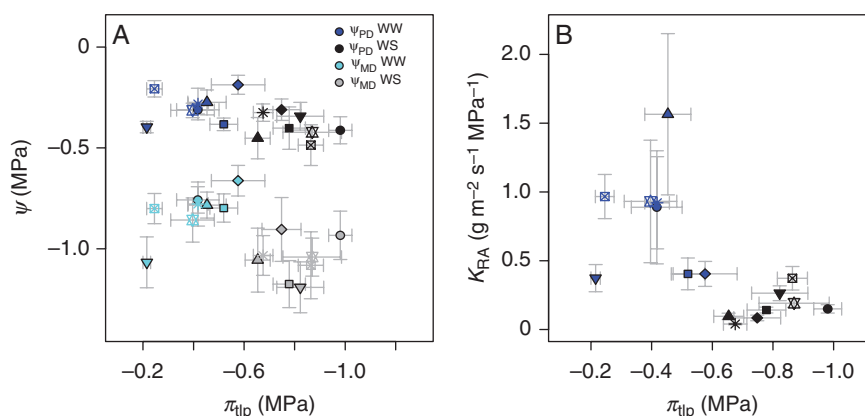


FIG. 7. Examples of the relationships between the root p–v curve traits (here, turgor loss point;  $\pi_{tip}$ ) and plant water stress, measured here as pre-dawn and midday water potentials ( $\Psi_{pd}$  and  $\Psi_{md}$ ; A), and hydraulics, measured as whole-plant conductance normalized by root system area ( $K_{RA}$ ; B). Symbols follow Fig. 3, except that the darker symbols in (A) represent  $\Psi_{pd}$  and the lighter symbols represent  $\Psi_{md}$ .  $n = 5$ –11 roots for the p–v traits;  $n = 3$  plants for  $\Psi$  and  $K_{RA}$ . Water stress reduced plant water potentials and hydraulic conductance, but these variables were not associated with the root traits (Supplementary data Table S2).

that previous field trials classified as drought tolerant, based on canopy growth in dry conditions, exhibited significantly lower trait values in well-watered, but not water-stressed, conditions, contrary to expectation (Fig. 8). Altogether, these findings show that root p–v traits are important to gas exchange and water uptake from dry soil and suggest that maintaining root turgor and volume also contributes to drought tolerance in field conditions, potentially by enabling greater water uptake from deeper, wetter soil. Therefore, characterizing these traits is a promising approach to capture diversity in below-ground drought tolerance.

#### Biophysical interpretations and mechanistic drivers of the root p–v traits

Pressure–volume analyses were developed for leaves, and two main structural differences could change the physiological interpretations of the p–v curve traits in roots.

First, the root traits, measured here on 15–20 cm sections, represent the composite properties of tissues from several developmental zones, including the tip, maturation zone and

beginning of the secondary growth zone (Gambetta et al., 2013). Organ trait values are assumed to represent a weighted average of tissue traits, but modelling the effects of tissue heterogeneity indicates that turgor loss from the most vulnerable tissues can generate curve inflection points, which are used to graphically define  $\pi_{tip}$  and RWC<sub>tip</sub>, even though turgor is still positive in the less vulnerable tissues (Cheung et al., 1976; Tyree, 1981). Thus, the root trait values could over-represent the properties of vulnerable cell types, such as root hairs. Further, measuring roots from similar developmental stages, with largely consistent proportions of primary (white, unsuberized) and secondary (woody) tissue, could be important to compare traits across cultivars or species, if these traits vary across root zones. We did not measure the proportion of these zones in the sampled roots, but we visually estimated that about a third of the root length was unsuberized, consistently across rootstocks. Future work evaluating how p–v traits vary across zones could make root trait values more readily comparable across sites or studies by allowing values to be corrected by the proportion of root zones.

Second, in leaves, the curves are assumed to capture the properties of intact, dehydrating cells, while lacunae formation

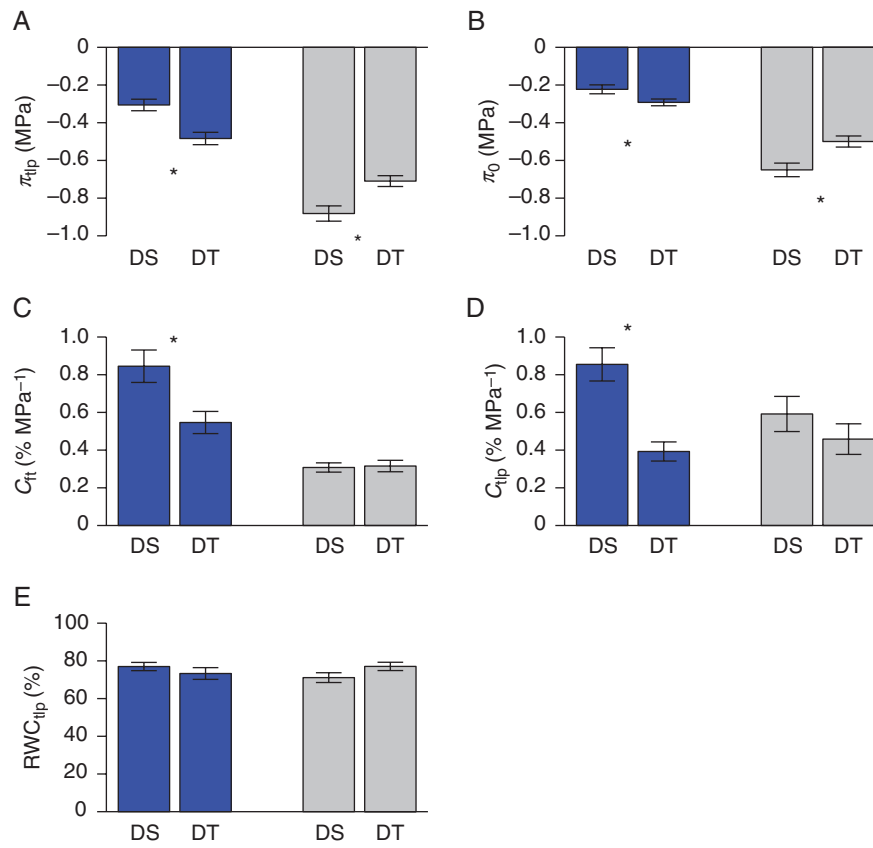


FIG. 8. Trait differences between the rootstocks that field trials have classified as drought tolerant (DT) (140Ru, 1103P, 110R and Ramsey) and drought sensitive (DS) (420A, 5C, Riparia Gloire and 101-14). Drought tolerance is defined here as a greater ability to maintain canopy growth (scion vigor) under deficit irrigation in vineyard conditions. Blue bars show the mean trait values for well-watered plants and grey bars show mean values for water-stressed plants. Error bars are standard errors.  $n = 24-30$  roots. Asterisks indicate significant differences. The drought-tolerant rootstocks exhibited a significantly lower  $\pi_{tip}$ ,  $\pi_0$ ,  $C_{ft}$  and  $C_{tip}$  under well-watered conditions, but  $C_{ft}$  and  $C_{tip}$  were not significantly different between drought-tolerant and drought-sensitive varieties under water stress, while  $\pi_{tip}$  and  $\pi_0$  were significantly less negative in the tolerant rootstocks under water stress, contrary to our expectations (A–D).

suggests curves for roots could also reflect relationships between  $\Psi$  and the volume of water released by cell implosion and rupture (Cheung *et al.*, 1975; Cuneo *et al.*, 2016, 2021). In 140-Ru, the  $\pi_{tip}$  in well-watered vines occurred within the range of water potentials initiating lacunae formation ( $\pi_{tip} = -0.45$  MPa, while lacunae occupied 0 % of root area at  $-0.3$  MPa and 12 % at  $-0.6$  MPa) (Cuneo *et al.*, 2016) (Fig. 2). We compare previous findings with well-watered trait values when plants are subjected to short droughts (<1 week), since root  $\pi_0$  typically requires at least a week to adjust to new conditions (Düring, 1984). Thus, root  $\pi_{tip}$  could measure  $\Psi$  at which the  $p-v$  relationship transitions from measuring water loss from intact cells to lacunae formation. The lack of significant lacunae formation prior to  $\pi_{tip}$  suggests that  $C_{ft}$  measures water loss from intact cells in both organs, but approx. 30 % of the root cortex developed lacunae by  $-1.2$  MPa, suggesting the water released by cell implosion could be important to root  $C_{tip}$  (Cuneo *et al.*, 2016).

Clarifying the biophysical interpretation of these traits, and identifying the drivers of trait diversity and adjustment, would provide crucial insight into the mechanisms that confer below-ground drought tolerance. The drivers of cell implosion are largely unknown, while wall stiffness is the main biochemical and structural driver of  $C_{ft}$  in leaves, with stiffer walls reducing

capacitance by restricting changes in cell volume (Bartlett *et al.*, 2012b; Nadal *et al.*, 2018). Cell wall thickness and chemical composition are closely related to stiffness, suggesting that wall structure and chemistry could drive variation in  $C_{ft}$  (Moore *et al.*, 2008; Peguero-Pina *et al.*, 2017). Many species increase cell wall thickness in their leaves under water stress (Cutler *et al.*, 1977), while grape leaves subjected to cold stress reduced their cell wall pectin content, which increased wall stiffness and reduced  $C_{ft}$  (Roig-Oliver *et al.*, 2020). Grape rootstocks vary in suberin deposition in the cell walls in the maturation and secondary growth zones under water stress, but  $C_{ft}$  was not significantly different between varieties that exhibited greater (101-14) or less suberization (110R) (Barrios-Masias *et al.*, 2015). Other crop species have been shown to alter polysaccharide composition in the root cell walls during drought (Piro *et al.*, 2003). Also, trait adjustment in water-stressed plants could reflect biophysical differences between the tissues developed under wet and dry conditions, or differences between previously unstressed tissues, without lacunae, and tissues composed of only the cells that remain after the vulnerable cells have imploded. Further work is needed to determine how lacunae formation and cell structure and biochemistry in different developmental zones impact diversity and adjustment in these traits; however, regardless, this study shows that

these traits hold promise for characterizing rootstock drought tolerance.

#### *Potential mechanisms relating root capacitance to gas exchange during drought*

Several mechanisms could drive the association between lower root capacitance and greater gas exchange under water stress. First, the rootstocks with a lower capacitance could maintain greater hydraulic function. Cell shrinkage in the root maturation zone under water stress would reduce the contact between roots and soil and, thus, the hydraulic conductance at the soil–root interface, while lacunae formation would reduce the hydraulic conductance across the root cortex (North and Nobel, 1997; Carminati et al., 2009; Cuneo et al., 2016). Since capacitance measures the decline in root volume with water potential, a lower capacitance could indicate that the roots retain more volume in the maturation zone, via less cell shrinkage or lacunae formation, and thus maintain greater contact with the soil, hydraulic conductance and water transport. However, capacitance was not correlated with  $K_{\text{plant}}$  or  $K_{\text{RA}}$  (Fig. 7), and a short dry-down produced stronger declines in root hydraulic conductivity in 110R than in 101-14 (Cuneo et al., 2021), which exhibited similar capacitance values in well-watered plants (Fig. 1; Supplementary data Fig. S3).

Alternatively, capacitance could impact gas exchange through root to shoot signalling. Grape rootstocks vary in ABA content under water stress, and root ABA content was correlated with stomatal closure during drought across multiple rootstocks grafted to the same scion variety (Soar et al., 2006; Speirs et al., 2013; Rossedeutsch et al., 2016). In maize, cells in all root zones generated ABA under drought, and ABA production was proportional to the percentage decline in root volume (Zhang and Tardieu, 1996). These findings suggest that the rootstocks with a lower capacitance could maintain greater gas exchange under water stress through smaller declines in root volume and less ABA production. Notably, Rossedeutsch et al. (2016) measured ABA production during drought for four rootstocks from this study, and Riparia and 140-Ru exhibited both significantly higher root ABA concentrations and  $C_{\text{R}}$  values than 101-14 and 110R (Fig. 2). However, contrary to this hypothesis, work in other species suggests that stomata mainly respond to leaf ABA production (McAdam et al., 2016), while root ABA content is more strongly determined by basipetal transport than endogenous root production (Manzi et al., 2015). ABA is also not strongly upregulated in grape leaves until the stomata are mostly closed, which would not produce the moderate declines in  $g_s$  observed here (Tombesi et al., 2015; Rodriguez-Dominguez et al., 2016; Gambetta et al., 2020) (Fig. 3; Supplementary data Fig. S4).

Finally, root capacitance could be related to gas exchange through effects on water storage dynamics in the secondary growth zone. However, a higher capacitance would be expected to increase gas exchange, since storage tissues with a larger capacitance would release more water as plant water potentials decline, increasing the water available for gas exchange (Meinzer et al., 2004; Bartlett et al., 2019; Strock and Lynch, 2020). Our findings showing the opposite suggest that other

mechanisms drive this relationship. Further work is needed to evaluate potential mechanisms by determining the impacts of p–v traits on root hydraulics and signalling.

#### *Potential mechanisms linking root p–v traits to drought tolerance in field conditions*

Adjusting to a lower capacitance increased water uptake from dry soil in this greenhouse experiment, but the trait differences between rootstocks classified as drought tolerant or sensitive by field trials suggest that these traits contribute to drought tolerance in the field by increasing water depletion from wetter soil zones. Grapevines are deeply rooted, with >25 % of root biomass typically distributed below 1 m, and thus experience wet conditions in deep soil and recurring cycles of drought and irrigation at the surface at the same time (Araujo et al., 1995; Smart et al., 2006). The trait differences between tolerant and sensitive rootstocks (Fig. 8) suggest that the tolerant rootstocks would exhibit a lower  $\pi_{\text{tip}}$ ,  $\pi_{\text{o}}$ ,  $C_{\text{R}}$  and  $C_{\text{tip}}$  in the roots in wetter and deeper soil, and a higher  $\pi_{\text{tip}}$  and  $\pi_{\text{o}}$  in the droughted roots at the surface. Thus, tolerant rootstocks could maintain greater turgor and volume in deeper roots but lose more turgor from surface roots, as the roots deplete the surrounding soil to more negative water potentials. These trait values could improve hydraulic function and facilitate growth in deeper roots for the tolerant rootstocks (Frensch and Hsiao, 1994; Gambetta et al., 2012). Drought-tolerant rootstocks exhibit more root growth in wet soil, including deeper soil layers and re-irrigated soil following drought (Alsina et al., 2011; Fort et al., 2017; Cuneo et al., 2021), and lower p–v curve trait values were significantly associated with a larger root area (Table 3; Fig. 6). Further, counterintuitively, limiting osmotic adjustment in dry surface roots could contribute to tolerance by concentrating resources on deep root proliferation. Osmotic adjustment would strengthen the water potential gradient driving hydraulic redistribution from hydrated to droughted roots, which has been shown to reduce mortality for grape roots in dry soil (Smart et al., 2005; Bauerle et al., 2008b). Root respiration is a significant carbon cost for grapevines, accounting for up to 40 % of photosynthesis (Escalona et al., 2012). Thus, limiting adjustment could facilitate deep root proliferation and increase access to soil water by reducing carbon allocation to dry surface roots. Future work is needed to determine whether p–v curve traits contribute to rootstock differences in root growth and distribution.

#### Conclusions

These findings are the first to show that root p–v curve traits are important to plant drought tolerance. The rootstocks with a lower capacitance maintained greater gas exchange under water stress, suggesting that adjustment in root structure and biochemistry to retain greater root volume could improve below-ground hydraulic function under drought. However, the trait values measured for well-watered plants could be more important for drought tolerance in field conditions, where grapevines can use deep rooting to access wet soil, despite dry

conditions at the surface. These measurements are currently limited to roots with the mechanical strength to resist damage from the pressure bomb, which probably excludes herbaceous species. However, demonstrating that these traits are important to drought tolerance incentivizes future work to develop more versatile alternative methods, as for leaf  $p-v$  traits (e.g. Bartlett *et al.*, 2012a). Overall, these findings show that root  $p-v$  curve traits are a potentially powerful approach to characterize below-ground drought tolerance for diverse plants and provide phenotypic targets to improve crop drought tolerance.

#### SUPPLEMENTARY DATA

Supplementary data are available online at <https://academic.oup.com/aob> and consist of the following. Table S1: the best-fit models predicting the recovery in transpiration after re-watering. Table S2: the best-fit models predicting the pre-dawn and midday water potentials, whole-plant hydraulic conductance, and conductance normalized by root area. Figure S1: pot water contents over the course of the experimental period for each of the eight rootstock varieties. Figure S2: whole-plant transpiration over the course of the experiment for each rootstock. Figure S3: root pressure–volume curves for each of the eight rootstocks. Figure S4: midday stomatal conductance over the course of the experiment for each of the eight rootstocks. Figure S5: midday photosynthesis over the course of the experiment for each of the eight rootstocks. Figure S6: midday leaf water potential over the course of the experiment for each of the eight rootstocks. Figure S7: correlations between the whole-plant transpiration rates before and after re-watering to saturation.

#### ACKNOWLEDGEMENTS

M.K.B. led designing and performing the experiments, analysing the data, and writing the manuscript; M.A.W., A.J.M. and TK contributed to experimental design, data interpretation and manuscript preparation; T.K. also contributed the design for the canopy imaging platform and the protocol for the image analysis; G.S. and G.F. conducted the experiments and revised the manuscript.

#### FUNDING

This work was supported by the American Vineyard Foundation [#AVF-2284], the University of California, Davis College of Agricultural and Environmental Sciences and Department of Viticulture and Enology, and generous donations from the Rossi family to the department.

#### LITERATURE CITED

- Alsina MM, Smart DR, Bauerle T, *et al.* 2011. Seasonal changes of whole root system conductance by a drought-tolerant grape root system. *Journal of Experimental Botany* **62**: 99–109.
- Araujo F, Williams LE, Grimes DW, Matthews MA. 1995. A comparative study of young ‘Thompson Seedless’ grapevines under drip and furrow irrigation. I. Root and soil water distributions. *Scientia Horticulturae* **60**: 235–249.
- Barrios-Masias FH, Knipfer T, McElrone AJ. 2015. Differential responses of grapevine rootstocks to water stress are associated with adjustments in fine root hydraulic physiology and suberization. *Journal of Experimental Botany* **66**: 6069–6078.
- Bartlett MK, Scoffoni C, Ardy R, *et al.* 2012a. Rapid determination of comparative drought tolerance traits: using an osmometer to predict turgor loss point. *Methods in Ecology and Evolution* **3**: 880–888.
- Bartlett MK, Scoffoni C, Sack L. 2012b. The determinants of leaf turgor loss point and prediction of drought tolerance of species and biomes: a global meta-analysis. *Ecology Letters* **15**: 393–405.
- Bartlett MK, Klein T, Jansen S, Choat B, Sack L. 2016. The correlations and sequence of plant stomatal, hydraulic, and wilting responses to drought. *Proceedings of the National Academy of Sciences, USA* **113**: 13098–13103.
- Bartlett MK, Detto M, Pacala SW. 2019. Predicting shifts in the functional composition of tropical forests under increased drought and CO<sub>2</sub> from trade-offs among plant hydraulic traits. *Ecology Letters* **22**: 67–77.
- Barton K. 2009. *Mu-MIn: Multi-model inference*. <https://cran.r-project.org/web/packages/MuMIn/index.html>
- Bauerle TL, Richards JH, Smart DR, Eissenstat DM. 2008a. Importance of internal hydraulic redistribution for prolonging the lifespan of roots in dry soil. *Plant, Cell & Environment* **31**: 177–186.
- Bauerle TL, Smart DR, Bauerle WL, Stockert C, Eissenstat DM. 2008b. Root foraging in response to heterogeneous soil moisture in two grapevines that differ in potential growth rate. *New Phytologist* **179**: 857–866.
- Bettiga LJ. 2003. *Wine grape varieties in California*. Oakland, CA: University of California, Agriculture and Natural Resources.
- Burnham KP, Anderson DR. 2010. *Model selection and multimodel inference: a practical information-theoretic approach*. New York: Springer.
- Carminati A, Vetterlein D, Weller U, Vogel H-J, Oswald SE. 2009. When roots lose contact. *Vadose Zone Journal* **8**: 805–809.
- Cheung YNS, Tyree MT, Dainty J. 1975. Water relations parameters on single leaves obtained in a pressure bomb and some ecological interpretations. *Canadian Journal of Botany* **53**: 1342–1346.
- Cheung YNS, Tyree MT, Dainty J. 1976. Some possible sources of error in determining bulk elastic moduli and other parameters from pressure–volume curves of shoots and leaves. *Canadian Journal of Botany* **54**: 758–765.
- Cuneo IF, Knipfer T, Brodersen CR, McElrone AJ. 2016. Mechanical failure of fine root cortical cells initiates plant hydraulic decline during drought. *Plant Physiology* **172**: 1669–1678.
- Cuneo IF, Barrios-Masias F, Knipfer T, *et al.* 2021. Differences in grapevine rootstock sensitivity and recovery from drought are linked to fine root cortical lacunae and root tip function. *New Phytologist* **229**: 272–283.
- Cutler JM, Rains DW, Loomis RS. 1977. The importance of cell size in the water relations of plants. *Physiologia Plantarum* **40**: 255–260.
- Dodson Peterson JC, Duncan R, Hirschfeld D, *et al.* 2019. Grape rootstock breeding and their performance based on the wolpert trials in California. In: Cantu D, Walker MA, eds. *Compendium of plant genomes. The grape genome*. Cham: Springer International Publishing, 301–318.
- Düring H. 1984. Evidence for osmotic adjustment to drought in grapevines (*Vitis vinifera* L.). *Vitis* **23**: 1–10.
- Escalona JM, Tomàs M, Martorell S, Medrano H, Ribas-Carbo M, Flexas J. 2012. Carbon balance in grapevines under different soil water supply: importance of whole plant respiration: carbon balance in grapevine. *Australian Journal of Grape and Wine Research* **18**: 308–318.
- Fort K, Fraga J, Grossi D, Walker MA. 2017. Early measures of drought tolerance in four grape rootstocks. *Journal of the American Society for Horticultural Science* **142**: 36–46.
- Frensch J, Hsiao TC. 1994. Transient responses of cell turgor and growth of maize roots as affected by changes in water potential. *Plant Physiology* **104**: 247–254.
- Gambetta GA, Manuck CM, Drucker ST, *et al.* 2012. The relationship between root hydraulics and scion vigour across *Vitis* rootstocks: what role do root aquaporins play? *Journal of Experimental Botany* **63**: 6445–6455.
- Gambetta GA, Fei J, Rost TL, *et al.* 2013. Water uptake along the length of grapevine fine roots: developmental anatomy, tissue-specific aquaporin expression, and pathways of water transport. *Plant Physiology* **163**: 1254–1265.
- Gambetta GA, Herrera JC, Dayer S, Feng Q, Hochberg U, Castellari SD. 2020. The physiology of drought stress in grapevine: towards an integrative definition of drought tolerance. *Journal of Experimental Botany* **71**: 4658–4676.

- Hsiao TC, Acevedo E, Fereres E, Henderson DW. 1976.** Water stress, growth, and osmotic adjustment. *Philosophical Transactions of the Royal Society B: Biological Sciences* **273**: 479–500.
- Jensen C, Henson I, Turner N. 1989.** Leaf gas exchange and water relations of lupins and wheat. II. Root and shoot water relations of lupin during drought-induced stomatal closure. *Functional Plant Biology* **16**: 415.
- Jordan PW, Nobel PS. 1984.** Thermal and water relations of roots of desert succulents. *Annals of Botany* **54**: 705–717.
- Kandiko RA, Timmis R, Worrall J. 1980.** Pressure–volume curves of shoots and roots of normal and drought conditioned western hemlock seedlings. *Canadian Journal of Forest Research* **10**: 10–16.
- Knipfer T, Eustis A, Brodersen C, Walker AM, McElrone AJ. 2015.** Grapevine species from varied native habitats exhibit differences in embolism formation/repair associated with leaf gas exchange and root pressure: contrasting response of wild grapevines to drought stress. *Plant, Cell & Environment* **38**: 1503–1513.
- Knipfer T, Reyes C, Momayyezi M, Brown PJ, Kluepfel D, McElrone AJ. 2020.** A comparative study on physiological responses to drought in walnut genotypes (RX1, Vlach, VX211) commercially available as rootstocks. *Trees* **34**: 665–678.
- Manzi M, Lado J, Rodrigo MJ, Zacarías L, Arbona V, Gómez-Cadenas A. 2015.** Root ABA accumulation in long-term water-stressed plants is sustained by hormone transport from aerial organs. *Plant & Cell Physiology* **56**: 2457–2466.
- McAdam SAM, Susmilch FC, Brodrribb TJ. 2016.** Stomatal responses to vapour pressure deficit are regulated by high speed gene expression in angiosperms: rapid ABA biosynthesis during VPD transition. *Plant, Cell & Environment* **39**: 485–491.
- Meinzer FC, James SA, Goldstein G. 2004.** Dynamics of transpiration, sap flow and use of stored water in tropical forest canopy trees. *Tree Physiology* **24**: 901–909.
- Moore JP, Vitré-Gibouin M, Farrant JM, Driouich A. 2008.** Adaptations of higher plant cell walls to water loss: drought vs desiccation. *Physiologia Plantarum* **134**: 237–245.
- Nadal M, Flexas J, Gulías J. 2018.** Possible link between photosynthesis and leaf modulus of elasticity among vascular plants: a new player in leaf traits relationships? *Ecology Letters* **21**: 1372–1379.
- Nakagawa S, Schielzeth H. 2013.** A general and simple method for obtaining  $R^2$  from generalized linear mixed-effects models. *Methods in Ecology and Evolution* **4**: 133–142.
- North GB, Nobel PS. 1995.** Hydraulic conductivity of concentric root tissues of *Agave deserti* Engelm. under wet and drying conditions. *New Phytologist* **130**: 47–57.
- North GB, Nobel PS. 1997.** Root–soil contact for the desert succulent *Agave deserti* in wet and drying soil. *New Phytologist* **135**: 21–29.
- Peguero-Pina JJ, Sancho-Knapik D, Gil-Pelegrín E. 2017.** Ancient cell structural traits and photosynthesis in today's environment. *Journal of Experimental Botany* **68**: 1389–1392.
- Piro G, Leucci MR, Waldron K, Dalessandro G. 2003.** Exposure to water stress causes changes in the biosynthesis of cell wall polysaccharides in roots of wheat cultivars varying in drought tolerance. *Plant Science* **165**: 559–569.
- Pita P, Pardos JA. 2001.** Growth, leaf morphology, water use and tissue water relations of *Eucalyptus globulus* clones in response to water deficit. *Tree Physiology* **21**: 599–607.
- Rodriguez-Dominguez CM, Brodrribb TJ. 2020.** Declining root water transport drives stomatal closure in olive under moderate water stress. *New Phytologist* **225**: 126–134.
- Rodriguez-Dominguez CM, Buckley TN, Egea G, et al. 2016.** Most stomatal closure in woody species under moderate drought can be explained by stomatal responses to leaf turgor. *Plant, Cell & Environment* **39**: 2014–2026.
- Rodriguez-Dominguez CM, Carins Murphy MR, Lucani C, Brodrribb TJ. 2018.** Mapping xylem failure in disparate organs of whole plants reveals extreme resistance in olive roots. *New Phytologist* **218**: 1025–1035.
- Roig-Oliver M, Nadal M, Clemente-Moreno MJ, Bota J, Flexas J. 2020.** Cell wall components regulate photosynthesis and leaf water relations of *Vitis vinifera* cv. Grenache acclimated to contrasting environmental conditions. *Journal of Plant Physiology* **244**: 153084.
- Rosdeusch L, Edwards E, Cookson SJ, et al. 2016.** ABA-mediated responses to water deficit separate grapevine genotypes by their genetic background. *BMC Plant Biology* **16**: 91.
- Sack L, Pasquet-Kok J. 2011.** Leaf pressure–volume curves. <https://prometheuswiki.rsb.anu.edu.au/tiki-index.php?page=Leaf+pressure+volume+curve+parameters>.
- Schneider CA, Rasband WS, Eliceiri KW. 2012.** NIH Image to ImageJ: 25 years of image analysis. *Nature Methods* **9**: 671–675.
- Smart DR, Carlisle E, Goebel M, Nunez BA. 2005.** Transverse hydraulic redistribution by a grapevine. *Plant, Cell & Environment* **28**: 157–166.
- Smart DR, Schwass E, Lakso A, Morano L. 2006.** Grapevine rooting patterns: a comprehensive analysis and a review. *American Journal of Enology and Viticulture* **57**: 89–104.
- Soar CJ, Dry PR, Loveys BR. 2006.** Scion photosynthesis and leaf gas exchange in *Vitis vinifera* L. cv. Shiraz: mediation of rootstock effects via xylem sap ABA. *Australian Journal of Grape and Wine Research* **12**: 82–96.
- Speirs J, Binney A, Collins M, Edwards E, Loveys B. 2013.** Expression of ABA synthesis and metabolism genes under different irrigation strategies and atmospheric VPDs is associated with stomatal conductance in grapevine (*Vitis vinifera* L. cv Cabernet Sauvignon). *Journal of Experimental Botany* **64**: 1907–1916.
- Steudle E, Peterson CA. 1998.** How does water get through roots? *Journal of Experimental Botany* **49**: 775–788.
- Strock CF, Lynch JP. 2020.** Root secondary growth: an unexplored component of soil resource acquisition. *Annals of Botany* **126**: 205–218.
- Tombesi S, Nardini A, Frioni T, et al. 2015.** Stomatal closure is induced by hydraulic signals and maintained by ABA in drought-stressed grapevine. *Scientific Reports* **5**: 12449.
- Tsuda M, Tyree MT. 1997.** Whole-plant hydraulic resistance and vulnerability segmentation in *Acer saccharinum*. *Tree Physiology* **17**: 351–357.
- Turner NC, Stern WR, Evans P. 1987.** Water relations and osmotic adjustment of leaves and roots of lupins in response to water deficits. *Crop Science* **27**: 977–983.
- Tyree MT. 1981.** The relationship between the bulk modulus of elasticity of a complex tissue and the mean modulus of its cells. *Annals of Botany* **47**: 547–559.
- Westgate ME, Boyer JS. 1985.** Osmotic adjustment and the inhibition of leaf, root, stem and silk growth at low water potentials in maize. *Planta* **164**: 540–549.
- Zhang J, Tardieu F. 1996.** Relative contribution of apices and mature tissues to ABA synthesis in droughted maize root systems. *Plant & Cell Physiology* **37**: 598–605.